EVOLUTIONARY BIOLOGY

Carbon isotope evidence for the global physiology of Proterozoic cyanobacteria

Sarah J. Hurley[1,2]*, Boswell A. Wing[1], Claire E. Jasper[1], Nicholas C. Hill[2,3], Jeffrey C. Cameron[2,3,4]*

Ancestral cyanobacteria are assumed to be prominent primary producers after the Great Oxidation Event [≈2.4 to 2.0 billion years (Ga) ago], but carbon isotope fractionation by extant marine cyanobacteria (α-cyanobacteria) is inconsistent with isotopic records of carbon fixation by primary producers in the mid-Proterozoic eon (1.8 to 1.0 Ga ago). To resolve this disagreement, we quantified carbon isotope fractionation by a wild-type planktic β-cyanobacterium (*Synechococcus* sp. PCC 7002), an engineered Proterozoic analog lacking a CO_2-concentrating mechanism, and cyanobacterial mats. At mid-Proterozoic pH and pCO_2 values, carbon isotope fractionation by the wild-type β-cyanobacterium is fully consistent with the Proterozoic carbon isotope record, suggesting that cyanobacteria with CO_2-concentrating mechanisms were apparently the major primary producers in the pelagic Proterozoic ocean, despite atmospheric CO_2 levels up to 100 times modern. The selectively permeable microcompartments central to cyanobacterial CO_2-concentrating mechanisms ("carboxysomes") likely emerged to shield rubisco from O_2 during the Great Oxidation Event.

INTRODUCTION

Members of the phylum Cyanobacteria are the only extant bacteria capable of oxygenic photosynthesis, leading to the inference that ancestral cyanobacteria were responsible for the Paleoproterozoic accumulation of atmospheric O_2 known as the Great Oxidation Event [GOE; 2.4 to 2.0 billion years (Ga) ago] (*1*). Although estimates of when oxygenic photosynthesis originated span a billion years—from sometime in the Paleoarchean eon (3.6 to 3.2 Ga ago) to immediately preceding the GOE [Fig. 1 and the Supplementary Materials (SM)] [e.g., (*2*, *3*)]—the oxidative impact of this metabolism across the GOE was profound. Atmospheric O_2 concentrations increased by up to 100 million–fold (*1*, *4*) relative to CO_2 concentrations (Fig. 1), while primary productivity rose to potentially modern levels (*5*). Following the GOE, the trajectories of both atmospheric O_2 concentrations and primary productivity appear to have stalled, with atmospheric oxygen falling to somewhere between 0.1 and 10% of present atmospheric levels [1 PAL = 210,000 parts per million (ppm) O_2; Fig. 1] (*1*, *6*) and oxygenic primary production decreasing to less than 10% of modern values (*5*). Stabilization of the Earth system at this intermediate state of oxygenic primary production characterized much of the Proterozoic eon (*7*, *8*). There are a variety of hypotheses for why this stasis defined the Proterozoic Earth system [e.g., (*9*–*12*)] and the physiology of ancestral cyanobacteria features prominently in all of them.

While ancestral cyanobacteria are assumed to play a central role in Proterozoic biogeochemistry, there is limited direct evidence of the ecological niches that they occupied. The oldest unambiguous cyanobacterial microfossils are found in 2.018- to 2.015-Ga peritidal black cherts of the Orosirian Belcher Group (*13*, *14*). When similarly preserved fossil cyanobacteria are found in younger Proterozoic rocks, they are also interpreted as ancient analogs of benthic cyanobacteria in littoral environments (*15*). If the paleontological record is expanded to include all possible microfossils with cyanobacterial affinities, then benthic forms still dominate, with rare and contentious interpretations of cyanobacteria in planktic habitats (*16*, *17*). The lack of fossil indicators for planktic cyanobacteria may reflect an absence of these cyanobacterial lineages at this time (*18*) or the improbable preservation of cyanobacterial microfossils in pelagic environments (*19*). Paired biomarker and nitrogen isotope measurements identify the presence of pelagic cyanobacteria by 1.1 Ga ago (*20*), but earlier documentation of a pelagic habitat would help evaluate hypotheses for the global influence of cyanobacteria in the Proterozoic Earth system.

If Proterozoic cyanobacteria inhabited a globally important ecological niche, the productivity of the biosphere would be largely dependent on their ability to fix carbon. At the level of the global marine ecosystem, the most continuous evidence of carbon fixation by the dominant primary producers is preserved in sedimentary marine carbon isotope records. The carbon isotopic difference between carbonate minerals and total organic carbon (TOC) (ε_{TOC}; eq. S1) in sedimentary rocks has well-resolved coverage between the GOE, the origin of photosynthetic eukaryotes (*21*), and the ultimate ecological dominance of photosynthetic eukaryotes in the pelagic marine environment (*22*). Although the isotopic difference summarized by ε_{TOC} is imparted initially by the net carbon isotope effect associated with carbon fixation by primary producers (ε_P; eq. S2), carbon isotope fractionations associated with geologic preservation do not allow for ε_{TOC} to be directly substituted for ε_P (*23*).

We used bootstrap resampling and Monte Carlo simulations to produce a new record of ε_P in the middle of the Proterozoic eon (1.8 to 1.0 Ga ago), taking into account isotopic fractionations that occur as the primary substrates and products of carbon fixation (e.g., dissolved CO_2 and photoautotrophic biomass) are transformed into their final geological states (e.g., carbonate rocks and TOC). This new ε_P record was derived from a curated dataset of carbon isotope measurements from sedimentary rocks from a variety of depositional settings, including open and shallow marine environments (*24*). The middle Proterozoic shows limited variation in the sedimentary carbon isotope record [e.g., (*8*, *24*)] spanning the proposed "Age of Cyanobacteria" (*25*). As a result, it represents a favorable target for isolation of any cyanobacterial component of the Proterozoic ε_P record.

[1]Department of Geological Sciences, University of Colorado Boulder, Boulder, CO 80302, USA. [2]Renewable and Sustainable Energy Institute, University of Colorado, Boulder, CO 80309, USA. [3]Department of Biochemistry, University of Colorado, Boulder, CO 80309, USA. [4]National Renewable Energy Laboratory, Golden, CO 80401, USA.
*Corresponding author. Email: sarah.hurley@colorado.edu (S.J.H.); jeffrey.c.cameron@colorado.edu (J.C.C.)

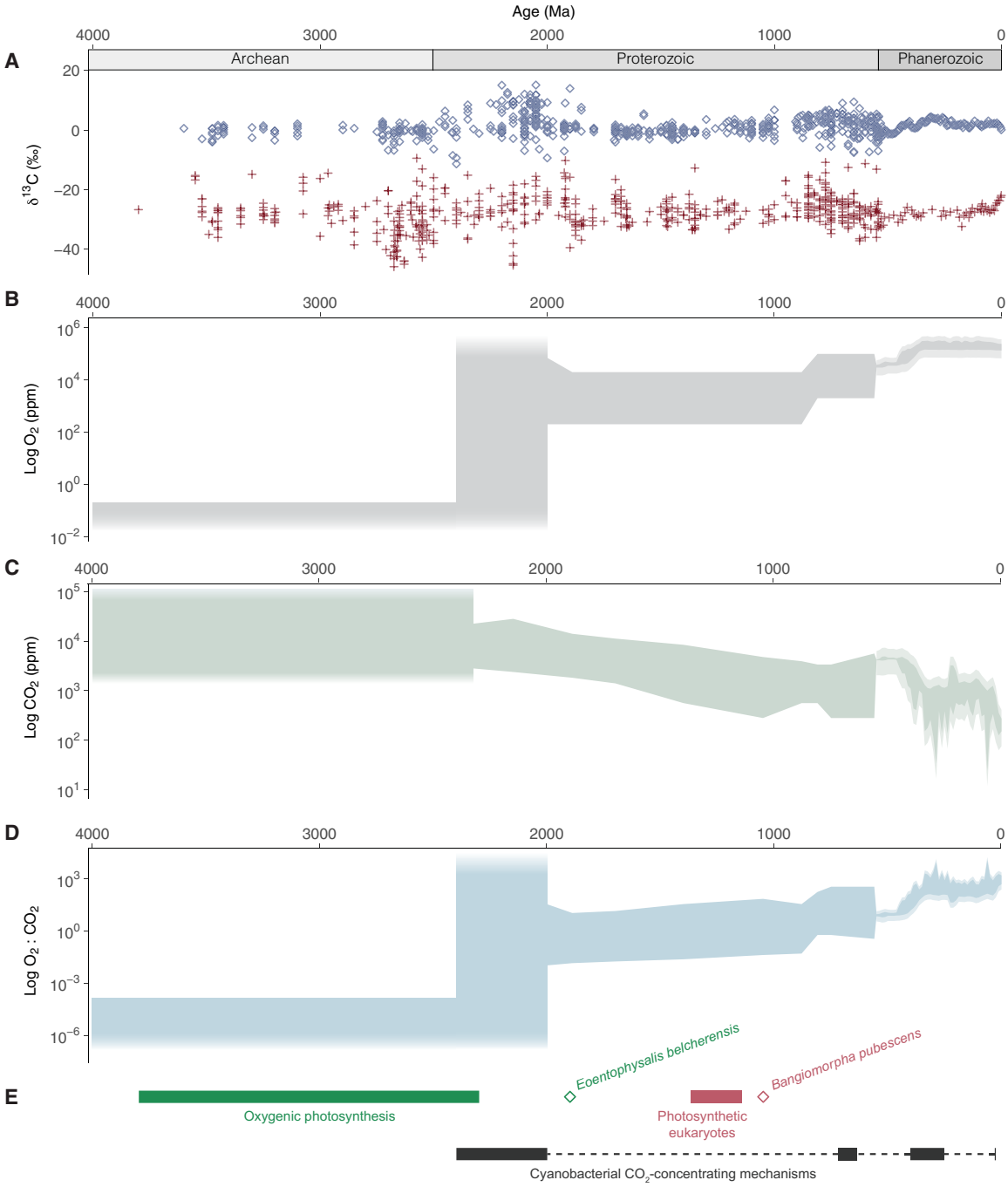

Fig. 1. Isotopic, atmospheric, and biologic context for the Proterozoic "Age of Cyanobacteria" (*25*). (**A**) Carbonate $\delta^{13}C$ values shown in blue diamonds and total organic carbon $\delta^{13}C$ values shown in red crosses (*24*). Ma, million years. (**B**) Mass-independent sulfur isotope fractionation restricts Archean pO_2 estimates to $<10^{-6}$ PAL or 2 ppm (*4*). Proterozoic and Phanerozoic pO_2 estimates come from proxies and modeling (*8*, *39*, *59*). (**C**) Archean, Proterozoic, and Phanerozoic CO_2 estimates come from proxies and modeling (*8*, *39*, *59*). (**D**) Estimated range of O_2-to-CO_2 ratios (each expressed in ppm) from the Archean through the Phanerozoic eons. (**E**) Range of time estimates for the origin of oxygenic photosynthesis (e.g., *2*, *3*) shown as a green bar and the earliest unambiguous cyanobacterial microfossils (*Eoentophysalis belcherensis*) shown as a green diamond (*13*, *14*). Age of earliest unambiguous photosynthetic eukaryote (*Bangiomorpha pubescens*) shown as red diamond with corresponding molecular clock estimates for the primary plastid endosymbiosis shown as a red bar (*21*). Proposed dates for the emergence of a cyanobacterial CCM shown as black bars [e.g., (*34*)].

Our statistical simulation of middle Proterozoic ε_P values yielded a distribution in which 95% of the values fall between 8 and 24 per mil (‰) (95th percentile) with a median value of 16‰ (Fig. 2A and the SM). This ε_P distribution provides a benchmark to compare different autotrophic contributions to global Proterozoic primary production.

Benthic cyanobacteria have, for example, been proposed as ecologically important contributors to Proterozoic primary production (*18*). In modern cyanobacterial mats, benthic photoautotrophic biomass is commonly enriched in ^{13}C relative to biomass from planktic environments [e.g., (*26*, *27*)]. We used our statistical simulation

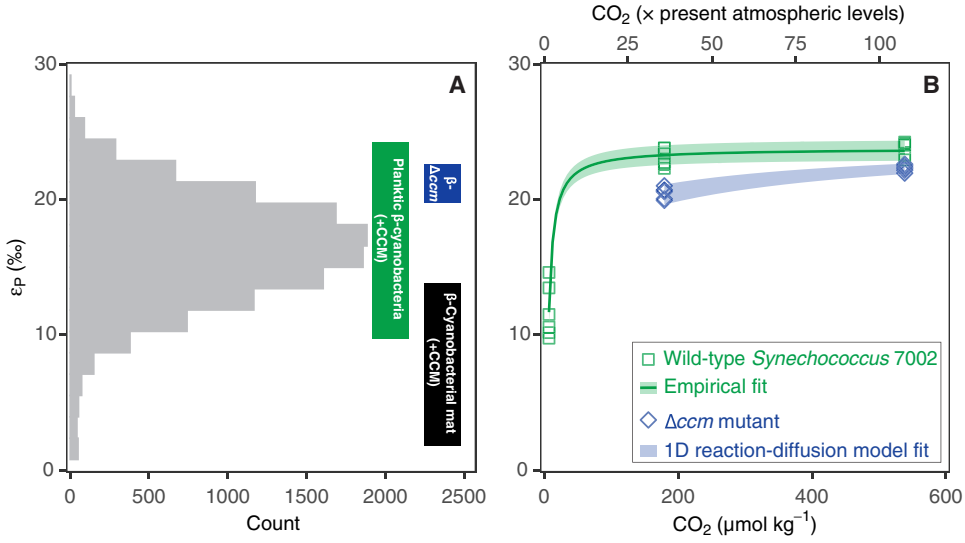

Fig. 2. Middle Proterozoic ε_P estimates as compared to empirical cyanobacterial ε_P values. (**A**) Histogram of estimated ε_P values between 1.0 and 1.8 Ga. Boxed vertical ranges represents ε_P values from a cyanobacterial mat system [black (*26*)] and ε_P values reported here in cultures of WT (green) and Δ*ccm* mutant (blue) *Synechococcus* sp. PCC 7002 strains. (**B**) Measured values of ε_P increase at higher dissolved CO_2 levels in cultures of *Synechococcus* sp. PCC 7002. In the WT strain (green squares), ε_P values covary with $[CO_{2(aq)}]^{-1}$ (green line, fig. S5; R^2, 0.96). Blue diamonds are experimental results for the Δ*ccm* mutant, which requires ≥36 × PAL CO_2 to grow under our experimental conditions. The shaded blue band represents calculations from a 1D reaction-diffusion model trained on physiological observations of the Δ*ccm* mutant. Horizontal axes refer to CO_2 in the culture headspace relative to PAL (1 PAL = 280 ppm CO_2; upper axis) and the corresponding dissolved CO_2 in the culture medium (micromole per kilogram; lower axis). Data points represent biological replicates (n = 6 for each condition).

to quantify the distribution of ε_P values in a well-characterized modern mat system on the basis of previously published values of $\delta^{13}C_{carb}$ and $\delta^{13}C_{org}$ (*26*). In this system, the predicted distribution of ε_P values has a median value of 8.5‰ and a range of 4 to 13‰ (95th percentile; fig. S3). This exercise suggests that the dynamics of carbon supply in cyanobacterial mats appears to limit the overall ε_P range that they can preserve, especially in hypersaline environments (*26*). The ε_P distribution for this system covers less than 25% of the middle Proterozoic ε_P record, with the overlap restricted to a small tail in the Proterozoic distribution that extends to ε_P values less than 10‰ (Fig. 2A). Detailed datasets do not exist that can similarly constrain how ε_P distributions for cyanobacterial mats might change if CO_2 levels approached those proposed for middle Proterozoic (*8*). Proof-of-concept experiments, however, indicate that mat ε_P values average ≈11‰ when overlying CO_2 levels are <36 × PAL (1 PAL = 280 ppm CO_2) and approach ≈25‰ only at CO_2 levels of ≈320 to 420 × PAL [table 2 in (*27*)]. Although benthic cyanobacterial microfossils are common in the Proterozoic eon, ε_P values associated with cyanobacterial mats appear to be much less than those seen in the middle Proterozoic ε_P distribution unless CO_2 levels were much greater than proposed for the middle Proterozoic (Fig. 2A).

The middle Proterozoic ε_P distribution also differs from ε_P values characteristic of planktic cyanobacteria dominant in open ocean ecosystems today (*28*). Values of ε_P cluster from ≈15 to 19‰ in physiologically controlled experiments with a planktic member of the monophyletic marine *Synechococcus/Prochlorococcus* (*Syn/Pro*) group (*28*), *Synechococcus* sp. CCMP838. This tight range spans less than 33% of the middle Proterozoic ε_P distribution. Experimental *Syn/Pro* ε_P values lack sensitivity to CO_2 levels [between 6 and 18 μmol kg^{-1} (*28*)] or specific growth rate (*28*), which suggests that variations in these factors cannot be called on to explain the full middle Proterozoic ε_P distribution. A complete interpretation of the Proterozoic carbon isotope record thus seems to require major contributions by noncyanobacterial primary producers or a shift in our understanding of carbon fixation by Proterozoic cyanobacteria.

It is possible that extant marine cyanobacteria from the *Syn/Pro* clade may not represent apt physiological analogs for Proterozoic cyanobacteria. All extant cyanobacteria use at least one CO_2-concentrating mechanism (CCM) (*29*) to increase the supply of CO_2 to rubisco (ribulose 1,5-bisphosphate carboxylase/oxygenase), the key CO_2-fixing enzyme in the Calvin-Benson cycle (*30*). Cyanobacterial rubisco is partitioned into a selectively permeable protein microcompartment known as a carboxysome along with carbonic anhydrase. Inside the carboxysome, actively accumulated intracellular HCO_3^- is rapidly interconverted into $CO_{2(aq)}$ through the activity of carbonic anhydrase (*29*, *31*, *32*). Examination of cyanobacterial CCMs reveals a clear division within the phylum (*29*). The marine *Syn/Pro* clade (α-cyanobacteria) contain α-carboxysomes and Form 1A rubisco that are evolutionarily (*29*) and structurally distinct (*29*, *33*) from the β-carboxysomes and form 1B rubisco shared by the freshwater, estuarine, and marine species (the β-cyanobacteria) in the remainder of the phylum.

As α-cyanobacteria diverged from cyanobacterial lineages of β-cyanobacteria at the end of the Proterozoic eon, between 1.0 and 0.5 Ga ago (*18*), β-carboxysomes appear to be the more ancient basis for a cyanobacterial CCM. Estimates for the initial emergence of CCMs in β-cyanobacteria span over 2 Ga of earth history (*34*) and are often associated with drops in global CO_2 associated with glacial episodes at ca. 2.4 to 2.0 Ga, ca. 0.7 to 0.6 Ga, and, potentially, 0.4 to 0.3 Ga ago (Fig. 1). It is possible that either biochemical differences between α- and β-cyanobacteria or the absence of β-carboxysomes in Proterozoic cyanobacteria could account for the mismatch between ε_P values from α-cyanobacteria and the middle Proterozoic ε_P distribution. Potential biochemical differences between α- and β-cyanobacteria include the influx and efflux of rubisco substrates

and products from the carboxysome (*33*) as well the kinetics of rubisco and carbonic anhydrase within the carboxysome (*35*). These differences would likely alter how whole-cell carbon fixation rates respond to changing environmental conditions (e.g., CO_2 concentrations), potentially expanding or contracting the accessible range of cyanobacterial ε_P values. The possible absence of a β-carboxysome in Proterozoic cyanobacteria would allow freer access of substrates to and from rubisco and carbonic anhydrase, potentially affecting cyanobacterial ε_P values over a wide range of CO_2 concentrations as well.

We propose that primary production by cyanobacteria in the middle Proterozoic might resemble either carbon fixation by extant cyanobacteria with β-carboxysome–based CCMs or a physiologically distinct mode of carbon fixation by ancestral β-cyanobacteria lacking a CCM. To evaluate these possibilities, we determined ε_P values for a model cyanobacterium containing β-carboxysomes, wild-type (WT) *Synechococcus* sp. PCC 7002 (*Synechococcus* 7002), and an engineered mutant of this strain lacking carboxysomes (Δ*ccm*) (*31*, *36*, *37*) across a range of CO_2 concentrations. Net carbon isotope fractionation by WT *Synechococcus* 7002 allows us to compare ε_P relationships in β-cyanobacteria to previously published ε_P values from α-cyanobacteria (fig. S6) (*28*). The Δ*ccm* mutant, which is high CO_2 requiring, represents a potential physiological analog for pre-CCM–bearing Proterozoic cyanobacteria.

RESULTS

WT *Synechococcus* 7002 grew at dissolved CO_2 concentrations of 7 to 538 μmol l^{-1}, corresponding to headspace CO_2 of 1 to 107 × PAL at pH 6.7 to 8.1. The Δ*ccm* mutant failed to grow at CO_2 levels of 1, 18, and 30 × PAL but was able to grow at 36 and 107 × PAL at pH 7.3 to 8.1 (fig. S4). These experimental conditions are consistent with both pCO_2 [1 to 100 PAL (*8*)] and pH [6.8 to 8.2 (*38*, *39*)] estimates relevant to the middle Proterozoic marine biosphere (fig. S10). The ε_P values from acclimated WT batch cultures range from 11.7 ± 2.0‰ to 23.8 ± 0.5‰ over 1 to 107 × PAL, while for Δ*ccm* batch cultures, ε_P values range from 20.5 ± 0.4 to 22.3 ± 0.2 over 36 to 107 × PAL (Fig. 2B). In both the WT and Δ*ccm* experiments, values of ε_P increase with higher concentrations of $CO_{2(aq)}$, in contrast to the insensitivity of ε_P to $CO_{2(aq)}$ in cyanobacteria with α-carboxysomes (fig. S6A) (*28*). The positive response of ε_P to increasing CO_2 concentrations indicates that transport limitation is a controlling factor in β-cyanobacterial carbon isotope fractionation, as has been well established for photosynthetic eukaryotes (fig. S6B) (*28*, *40*).

In WT *Synechococcus* 7002, ε_P values show a negative covariation with the inverse of dissolved CO_2 concentrations ($R^2 = 0.96$; figs. S5 and S6), further confirming similarities between cyanobacterial and algal net carbon isotope fractionation. Although the Δ*ccm* mutant did not grow over the full range of experimental CO_2 concentrations, it exhibits a 2.5-fold larger decrease in ε_P values over the same drop in CO_2 concentrations when compared to WT (≈1.8‰ versus ≈0.7‰ from 107 to 36 × PAL; Fig. 2B and fig. S5). These different CO_2 responses suggest that different mechanisms control CO_2 transport to rubisco in the Δ*ccm* mutant and WT strains.

To explore the isotopic response of the Δ*ccm* mutant to varying CO_2 concentrations, we used a one-dimensional (1D) reaction-diffusion model, in which rubisco is uniformly distributed throughout the cytosol (*31*). This model quantifies the isotopic consequences of the competition between a purely diffusional supply of $CO_{2(aq)}$ to the site of carbon fixation and CO_2 fixation into biomass, using three interdependent parameters: (i) the proportion of cellular surface area available for diffusion, (ii) the diffusion coefficient for $CO_{2(aq)}$ into the cell, and (iii) the distance over which $CO_{2(aq)}$ diffuses into the cell until it meets a free rubisco and is fixed (see the SM for detailed model description).

Modeled ε_P values for the Δ*ccm* mutant increase with respect to CO_2 concentrations (from ~20‰ at 36 × PAL to ~22‰ at 107 × PAL) with a slightly nonlinear functional dependence (Fig. 2B). Training the model on measured physiological parameters for the Δ*ccm* mutant illustrates the inefficiency of carbon fixation by rubisco relative to a purely diffusional supply of $CO_{2(aq)}$. To reproduce our ε_P-CO_2 observations, ≈70 to 90% of the carbon brought into a cyanobacterium without a carboxysome must be lost through back diffusion. This "leakiness" is calculated as the difference between the gross diffusive flux of CO_2 into the cell and the net rate of CO_2 fixation into biomass. The inability of the Δ*ccm* mutant to grow at CO_2 levels below 36 PAL during our experiments (Fig. 2B) was likely due to a combination of factors limiting the intracellular accumulation of CO_2, including the leakiness of the cell and the lack of an encapsulated carbonic anhydrase to convert accumulated HCO_3^- into CO_2 at the site of carbon fixation.

DISCUSSION

The distribution of ε_P values extracted from the middle Proterozoic sedimentary record span a range of 8 to 24‰ (95th percentile; Fig. 2A). If cyanobacteria accounted for the majority of primary production at this time, as is commonly asserted, then they should be able to produce a similar range of ε_P values. Our simulations of a previously characterized mat system (*26*) suggest that net carbon isotope fractionations by cyanobacteria in benthic settings may only account for the lower 25% of the middle Proterozoic ε_P distribution (Fig. 2A). Here, we show that net carbon isotope fractionation by β-cyanobacteria without carboxysomes only covers 13% of the middle Proterozoic ε_P distribution (Fig. 2A). In contrast, the ε_P range that we determined for planktic cyanobacteria with β-carboxysomes covers >90% of the middle Proterozoic distribution, suggesting that this physiology, in the appropriate ecological niches, could be responsible for a large proportion of Proterozoic primary production (Fig. 2A).

To understand whether evolutionary differences between extant and ancestral rubiscos might allow for β-cyanobacteria without carboxysomes to produce the full middle Proterozoic ε_P range, we used the Δ*ccm* model to calculate the ε_P relationships that might characterize β-cyanobacteria lacking carboxysomes with ancestral rubisco under middle Proterozoic CO_2 levels. We incorporated middle Proterozoic estimates of O_2 concentrations [0.1 to 10% PAL, compiled in (*8*)] in these model simulations as well. Although the timing of evolutionary changes within the rubisco phylogeny remains unconstrained (*41*), maximum carboxylation rates for ancestral variants of form 1B rubisco are ~50 to 70% of their modern equivalents, while the corresponding Menten constants for $CO_{2(aq)}$ are ~40 to 80% of their modern equivalents (*42*). Over a wide range of dissolved CO_2 and O_2 concentrations relevant to the Proterozoic ocean, our calculations suggest that a cyanobacterium without carboxysomes will exhibit a limited range of whole-cell ε_P values (<~10‰; Fig. 3 and the SM). While lower O_2 concentrations slightly contract the range of ε_P values (by ~3%) relative to those accessible at higher O_2 concentrations, the primary control seems to be the mismatch between a fast rate of

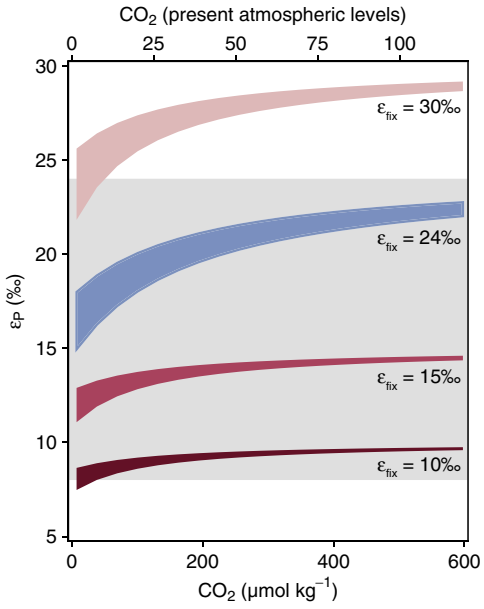

Fig. 3. Modeled relationships between ε_P and CO_2 concentration for β-cyanobacteria without a CCM incorporating estimated middle Proterozoic O_2 levels [0.1 to 10% PAL (*8*)]. The gray band represents the estimated middle Proterozoic distribution of ε_P values (95th percentile; 8 to 24‰). The blue field represents calculations extending the observed fractionation by the Δ*ccm* mutant across possible Proterozoic CO_2 and O_2 levels. The red fields represent calculations incorporating the measured kinetics of ancestral form 1B rubisco (table S3) (*42*) and the full range of known intrinsic isotope effects for rubisco (ε_{fix} = 10, 15, and 30‰; the SM).

CO_2 supply by diffusion and a slower rate of CO_2 fixation, which restricts the accessible range of net carbon isotope fractionation across all CO_2 levels in the modeled environment (Fig. 3). In this model, the absolute value of each ε_P range is set by the intrinsic carbon isotope fractionation factor assumed for rubisco (ε_{fix}; Fig. 3 and the SM). We note that resurrected forms of ancient rubisco have not yet been isotopically characterized. However, it appears that the lack of carboxysomes, rather than how reconstructed rubiscos ultimately fractionate carbon isotopes, restricts any one example of this physiological state from producing the full middle Proterozoic ε_P distribution.

The middle Proterozoic ε_P distribution ultimately reflects the interaction between the mode of carbon fixation and CO_2 supply for middle Proterozoic autotrophs. Estimates of middle Proterozoic atmospheric pCO_2 values range from 1 to 100 PAL (*8*), but the temporal and spatial resolution of these estimates is extremely coarse. The Our middle Proterozoic ε_P distribution encompasses a variety of marine environments and atmospheric conditions over the course of 800 million years, and therefore, pCO_2 and dissolved CO_2 could have exhibited wide variation in time and space over this interval. Estimates of pCO_2 over the past ≈70 million years, for example, span a relative range of ≈150-fold (60 to 8900 ppm by volume; https://www.paleo-co2.org), while dissolved CO_2 in the modern ocean varies over a relative range of ≈370-fold [8 to 2900 μmol kg^{-1} (*43*)]. If atmospheric or marine CO_2 in the middle Proterozoic varied similarly then planktic cyanobacteria with β-carboxysomes could produce the full range of middle Proterozoic ε_P values because of the strong dependence of their net carbon isotope fractionation on CO_2 concentrations (Fig. 2).

Although this inference does not rule out alternate forms of carbon fixation, the ranges of ε_P values produced by other plausible middle Proterozoic primary producers appear to be more restricted even when large variations in middle Proterozoic CO_2 concentrations are considered. In the case of β-cyanobacteria lacking CCMs, this is due to the slow rate of CO_2 fixation relative to the fast supply of CO_2 by diffusion, which restricts the ε_P response across different CO_2 concentrations (Fig. 3). Anoxygenic phototrophs lack carboxysomes (*44*), suggesting that their isotopic fractionation may show a similar lack of sensitivity to CO_2 concentrations as the Δ*ccm* mutant investigated here. In cyanobacterial mats, limited CO_2 supply appears to restrict ε_P to low values except, perhaps, when CO_2 levels are >300 PAL (*27*). Hypotheses that call on different carbon fixation modes to explain the middle Proterozoic ε_P distribution would therefore require the fortuitous preservation of the products of carbon fixation by a diversity of different primary producers.

We recognize that we cannot exclusively rule out these diversity hypotheses, but the genetic, biochemical, environmental, and physiological evidence discussed here points toward a prominent role for ancestral cyanobacteria with β-carboxysome–based CCMs in the middle Proterozoic biosphere. A Paleoproterozoic (or earlier) origin for the CCM in cyanobacteria is consistent with taphonomic inferences of late Mesoproterozoic biomineralization by CCM-bearing cyanobacteria (*45*). Cyanobacterial CCMs increase the access of rubisco to CO_2 to mitigate the enzyme's dual-substrate specificity for both CO_2 and O_2 [e.g., (*46*)]. Under the O_2-to-CO_2 ratios found in modern environments, competition between carboxylation and oxygenation reactions is metabolically expensive and imposes a wasteful loss of fixed carbon (*47*). Although Proterozoic pCO_2 estimates are higher than modern, spanning ~1 to 100 PAL [compiled in (*8*)], the jump in atmospheric O_2 across the GOE (*1*, *48*) increased the ratio of O_2 to CO_2 up to 100 million–fold (Fig. 1). These enhanced ratios were sustained throughout the Proterozoic at values at least four orders of magnitude greater than at the end of the Archean.

The transition to higher O_2-to-CO_2 ratios in the Proterozoic marine environment would have increased O_2-to-CO_2 ratios within Proterozoic cyanobacteria (*49*). The carboxysome may therefore have been an evolutionary innovation in response to extreme environmental oxygenation across the GOE. Despite being the principal component of the CCM in all cyanobacteria today, the carboxysome's original function may have been to shield rubisco from O_2 (*50*), after which it was repurposed as a CCM. This proposed function is consistent with predictions of limited CO_2 and O_2 permeation through the central pores of carboxysomal shell proteins (*33*). Early encapsulation inside of a dysoxic carboxysome could further explain why the specificity for CO_2 versus O_2 is lower in cyanobacterial form 1B rubisco than in form 1B rubisco from Archaeplastida (*51*), despite a common lineage [e.g., (*19*)] and over a billion years of shared environmental history (*21*).

Whether or not the carboxysome originated as an O_2-exclusion mechanism, its carbon isotope consequences appear to reach back at least 1.8 Ga (Fig. 2). Paleontological interpretations of ancestral cyanobacteria have long been rationalized in terms of morphological and local ecological stasis on geological time scales [e.g., (*52*)]. The observations reported here extend this working hypothesis of stasis to levels of biological organization—from the global marine ecosystem down to the organellar and, perhaps, biochemical realms—that have not been previously accessible to paleontological insight (*17*, *19*). When viewed in terms of the comprehensive nature of the Proterozoic carbon isotope record, this suggests that, like in the modern ocean, pelagic cyanobacteria were an important component

of Proterozoic marine primary productivity. If Proterozoic cyanobacteria were not strictly benthic forms restricted to littoral environments, then a range of hypotheses for limited primary productivity can be ruled out, from environmental hypotheses that rely on an inaccessible pelagic photic zone (*53*, *54*) to evolutionary hypotheses that posit a planktic lifestyle as a derived trait (*18*, *55*). The possibility that Proterozoic cyanobacteria so closely resembled an extant model cyanobacterium opens the door to direct testing of other hypotheses for limiting primary productivity [e.g., (*9*–*12*)] through new experiments in comparative physiology and competition under proposed Proterozoic environmental regimes. Cyanobacterial stasis in terms of ecology, morphology, cytology, and biochemistry may have been the foundation behind low Proterozoic productivity (*7*). The progressive increase of productivity through time could represent a stepwise scaling (*56*) away from this continuously maintained cyanobacterial state through the introduction of new avenues of primary production in the oceans (*19*) and, eventually, on land.

MATERIALS AND METHODS

Middle Proterozoic ε_P values

Our statistical simulations were based on bootstrap resampling of a curated dataset of $\delta^{13}C$ values of carbonate minerals and TOC in 1.0- to 1.8-Ga-old sedimentary rocks (*24*). We sampled uniform distributions representing possible C isotope fractionation during the conversion and preservation of dissolved CO_2 as carbonate minerals and primary biomass as TOC. The distribution of equilibrium isotope effects between $CO_{2\,(aq)}$ and HCO_3^- ($\varepsilon_{HCO_3^-\text{–}CO_{2\,(d)}}$) ranged from 8.9 to 11.7‰ (*57*) assuming photic zone temperatures of 3° to 30°C [e.g., (*38*)]. Experimentally determined kinetic isotope effects associated with the precipitation of calcite and aragonite relative to HCO_3^- ($\varepsilon_{cc-HCO_3^-}$) ranged from 0.8 to 3.3‰ (*58*). Carbon isotope fractionations associated with secondary biological processes such as heterotrophic consumption of primary organic matter ($\varepsilon_{reworking}$) ranged from 0 to 1.5‰ (*23*). Full simulations are detailed in the SM.

Culturing and isotope assays

Synechococcus sp. strain PCC 7002 (*Synechococcus* 7002) and a previously engineered Δ*ccm* mutant strain lacking a carboxysome were grown in A+ media, at 37°C under saturating light levels of ~227 ± 5 μmol photons m^{-2} s^{-1} provided by cool-white fluorescence lamps. Cultures were grown in 125-ml conical flasks with foam stoppers (Jaece Industries Identi-plug), continuously shaking, in an incubator that kept headspace CO_2 constant by continuous replacement with a mixture of CO_2 and air during each experiment. Headspace CO_2 varied across three experimental conditions: 0.04% (v/v) CO_2 (air), 1% (v/v) CO_2, and 3% (v/v) CO_2, corresponding to $CO_{2(aq)}$ concentrations of 7, 180, and 538 μmol kg^{-1}, respectively. At each CO_2 condition, strains were acclimated through the serial inoculation of four consecutive cultures. Each culture grew to an optical density at 730 nm of ~0.2 before inoculating the next culture with 1 to 3% of the final cell density and harvesting biomass. Harvested biomass was kept at −70°C, then centrifuged, and washed twice with ultrapurified water before isotopic analysis. Carbon isotope compositions of biomass were determined by first combusting samples in a Thermo Fisher Scientific FlashEA under a flow of He gas. The resultant CO_2 was analyzed with a Thermo Fisher Scientific Delta V Isotope Ratio Mass Spectrometer in continuous-flow mode. Carbon isotope compositions are expressed as the relative per mil difference between the ratio of ^{13}C-^{12}C in the sample ($^{13}C/^{12}C_{sample}$) and a standard of Vienna Pee Dee Belemnite ($^{13}C/^{12}C_{VPBD}$). Headspace CO_2 gas was purified and analyzed with a Thermo Fisher Scientific 253+ Isotope Ratio Mass Spectrometer in dual-inlet mode.

One-dimensional reaction-diffusion model

A full model description is in the SM. We used a 1D model of steady-state diffusion of CO_2 between an infinite extracellular source and an intracellular sink to represent rubisco-catalyzed entry of CO_2 into the Calvin-Benson cycle. A fixed distance separates the CO_2 source and enzymatic sink. Both the diffusive transport and the sink reaction are isotopically selective. Independent model inputs include the carbon fixation rates observed for the Δ*ccm* mutant grown under 1 and 3% CO_2 headspace, the calculated concentration of dissolved CO_2, and fractionation factors for form 1B rubisco (ε_{fix}) and diffusion of CO_2 in solution (ε_{diff}). The model has three free parameters: (i) the intracellular distance over which $CO_{2(aq)}$ diffuses, (ii) the intracellular diffusion coefficient for $CO_{2(aq)}$, and (iii) the proportion of cellular surface area available for diffusion. We "trained" the model by selecting interdependent sets of these three parameters that could reproduce experimental ε_P values at the observed carbon fixation rates in the Δ*ccm* mutant. In the trained model, we additionally used previously characterized kinetics of extant rubiscos and reconstructed ancestral rubiscos to determine possible ε_P values in β-cyanobacteria without a CCM over a range of environmental conditions.

SUPPLEMENTARY MATERIALS

Supplementary material for this article is available at http://advances.sciencemag.org/cgi/content/full/7/2/eabc8998/DC1

View/request a protocol for this paper from *Bio-protocol*.

REFERENCES AND NOTES

1. D. E. Canfield, The early history of atmospheric oxygen: Homage to Robert M. Garrels. *Annu. Rev. Earth Planet. Sci.* **33**, 1–36 (2005).
2. W. W. Fischer, J. Hemp, J. E. Johnson, Evolution of oxygenic photosynthesis. *Annu. Rev. Earth Planet. Sci.* **44**, 647–683 (2016).
3. P. Sánchez-Baracaldo, T. Cardona, On the origin of oxygenic photosynthesis and Cyanobacteria. *New Phytol.* **225**, 1440–1446 (2020).
4. D. C. Catling, K. J. Zahnle, The Archean atmosphere. *Sci. Adv.* **6**, eaax1420 (2020).
5. M. S. W. Hodgskiss, P. W. Crockford, Y. Peng, B. A. Wing, T. J. Horner, A productivity collapse to end Earth's Great Oxidation. *Proc. Natl. Acad. Sci. U.S.A.* **116**, 17207–17212 (2019).
6. N. J. Planavsky, C. T. Reinhard, X. Wang, D. Thomson, P. McGoldrick, R. H. Rainbird, T. Johnson, W. W. Fischer, T. W. Lyons, Low mid-Proterozoic atmospheric oxygen levels and the delayed rise of animals. *Science* **346**, 635–638 (2014).
7. P. W. Crockford, J. A. Hayles, H. Bao, N. J. Planavsky, A. Bekker, P. W. Fralick, G. P. Halverson, T. H. Bui, Y. Peng, B. A. Wing, Triple oxygen isotope evidence for limited mid-Proterozoic primary productivity. *Nature* **559**, 613–616 (2018).
8. P. W. Crockford, M. Kunzmann, A. Bekker, J. Hayles, H. Bao, G. P. Halverson, Y. Peng, T. H. Bui, G. M. Cox, T. M. Gibson, S. Wörndle, R. Rainbird, A. Lepland, N. L. Swanson-Hysell, S. Master, B. Sreenivas, A. Kuznetsov, V. Krupenik, B. A. Wing, Claypool continued: Extending the isotopic record of sedimentary sulfate. *Chem. Geol.* **513**, 200–225 (2019).
9. M. A. Kipp, E. E. Stüeken, Biomass recycling and Earth's early phosphorus cycle. *Sci. Adv.* **3**, eaao4795 (2017).
10. S. L. Olson, C. T. Reinhard, T. W. Lyons, Cyanobacterial diazotrophy and Earth's delayed oxygenation. *Front. Microbiol.* **7**, 1526 (2016).
11. C. Scott, T. W. Lyons, A. Bekker, Y. Shen, S. W. Poulton, X. Chu, A. D. Anbar, Tracing the stepwise oxygenation of the Proterozoic ocean. *Nature* **452**, 456–459 (2008).
12. K. Ozaki, K. J. Thompson, R. L. Simister, S. A. Crowe, C. T. Reinhard, Anoxygenic photosynthesis and the delayed oxygenation of Earth's atmosphere. *Nat. Commun.* **10**, 3026 (2019).
13. H. J. Hofmann, Precambrian Microflora, Belcher Islands, Canada: Significance and systematics. *J. Paleo.* **50**, 1040–1073 (1976).
14. M. S. W. Hodgskiss, O. M. J. Dagnaud, J. L. Frost, G. P. Halverson, M. D. Schmitz, N. L. Swanson-Hysell, E. A. Sperling, New insights on the Orosirian carbon cycle, early

Cyanobacteria, and the assembly of Laurentia from the Paleoproterozoic Belcher Group. *Earth Planet. Sci. Lett.* **520**, 141–152 (2019).
15. L. C. Kah, A. H. Knoll, Microbenthic distribution of Proterozoic tidal flats: Environmental and taphonomic considerations. *Geology* **24**, 79–82 (1996).
16. V. N. Sergeev, M. Sharma, Y. Shukla, Proterozoic fossil cyanobacteria. *Palaeobotanist* **61**, 189–358 (2012).
17. C. F. Demoulin, Y. J. Lara, L. Cornet, C. François, D. Baurain, A. Wilmotte, E. J. Javaux, Cyanobacteria evolution: Insight from the fossil record. *Free Radic. Biol. Med.* **140**, 206–223 (2019).
18. P. Sánchez-Baracaldo, Origin of marine planktonic cyanobacteria. *Sci. Rep.* **5**, 17418 (2015).
19. A. H. Knoll, R. E. Summons, J. R. Waldbauer, J. E. Zumberge, The geological succession of primary producers in the oceans, in *Evolution of Primary Producers in the Sea* (Elsevier, 2007), pp. 133–163.
20. N. Gueneli, A. M. McKenna, N. Ohkouchi, C. J. Boreham, J. Beghin, E. J. Javaux, J. J. Brocks, 1.1-billion-year-old porphyrins establish a marine ecosystem dominated by bacterial primary producers. *Proc. Natl. Acad. Sci. U.S.A.* **115**, E6978–E6986 (2018).
21. T. M. Gibson, P. M. Shih, V. M. Cumming, W. W. Fischer, P. W. Crockford, M. S. W. Hodgskiss, S. Wörndle, R. A. Creaser, R. H. Rainbird, T. M. Skulski, G. P. Halverson, Precise age of *Bangiomorpha pubescens* dates the origin of eukaryotic photosynthesis. *Geology* **46**, 135–138 (2017).
22. J. J. Brocks, A. J. M. Jarrett, E. Sirantoine, C. Hallmann, Y. Hoshino, T. Liyanage, The rise of algae in Cryogenian oceans and the emergence of animals. *Nature* **548**, 578–581 (2017).
23. J. M. Hayes, H. Strauss, A. J. Kaufman, The abundance of ^{13}C in marine organic matter and isotopic fractionation in the global biogeochemical cycle of carbon during the past 800 Ma. *Chem. Geol.* **161**, 103–125 (1999).
24. J. Krissansen-Totton, R. Buick, D. C. Catling, A statistical analysis of the carbon isotope record from the Archean to Phanerozoic and implications for the rise of oxygen. *Am. J. Sci.* **315**, 275–316 (2015).
25. J. Schopf, M. Walter, in *The Biology of Cyanobacteria*, N. G. Carr, B. A. Whitton, Eds. (Blackwell, 1982), pp. 543–564.
26. M. Schidlowski, H. Gorzawski, I. Dor, Carbon isotope variations in a solar pond microbial mat: Role of environmental gradients as steering variables. *Geochim. Cosmochim. Acta* **58**, 2289–2298 (1994).
27. D. J. Des Marais, D. E. Canfield, The carbon isotope biogeochemistry of microbial mats, in *Microbial Mats: Structure, Development and Environmental Significance*, L. J. Stal, P. Caumette, Eds. (Springer Berlin Heidelberg, 1994), pp. 289–298.
28. B. N. Popp, E. A. Laws, R. R. Bidigare, J. E. Dore, K. L. Hanson, S. G. Wakeham, Effect of phytoplankton cell geometry on carbon isotopic fractionation. *Geochim. Cosmochim. Acta* **62**, 69–77 (1998).
29. B. D. Rae, B. M. Long, M. R. Badger, G. D. Price, Functions, compositions, and evolution of the two types of carboxysomes: Polyhedral microcompartments that facilitate CO_2 fixation in cyanobacteria and some proteobacteria. *Microbiol. Mol. Biol. Rev.* **77**, 357–379 (2013).
30. T. D. Sharkey, Discovery of the canonical Calvin–Benson cycle. *Photosynth. Res.* **140**, 235–252 (2019).
31. J. C. Cameron, S. C. Wilson, S. L. Bernstein, C. A. Kerfeld, Biogenesis of a bacterial organelle: The carboxysome assembly pathway. *Cell* **155**, 1131–1140 (2013).
32. N. C. Hill, J. W. Tay, S. Altus, D. M. Bortz, J. C. Cameron, Life cycle of a cyanobacterial carboxysome. *Sci. Adv.* **6**, eaba1269 (2020).
33. P. Mahinthichaichan, D. M. Morris, Y. Wang, G. J. Jensen, E. Tajkhorshid, Selective permeability of carboxysome shell pores to anionic molecules. *J. Phys. Chem. B* **122**, 9110–9118 (2018).
34. M. Giordano, J. Beardall, J. A. Raven, CO_2 concentrating mechanisms in algae: Mechanisms, environmental modulation, and evolution. *Annu. Rev. Plant Biol.* **56**, 99–131 (2005).
35. L. Whitehead, B. M. Long, G. D. Price, M. R. Badger, Comparing the in vivo function of α-carboxysomes and β-carboxysomes in two model cyanobacteria. *Plant Physiol.* **165**, 398–411 (2014).
36. G. C. Gordon, T. C. Korosh, J. C. Cameron, A. L. Markley, M. B. Begemann, B. F. Pfleger, CRISPR interference as a titratable, *trans*-acting regulatory tool for metabolic engineering in the cyanobacterium *Synechococcus sp.* strain PCC 7002. *Metab. Eng.* **38**, 170–179 (2016).
37. R. L. Clark, G. C. Gordon, N. R. Bennett, H. Lyu, T. W. Root, B. F. Pfleger, High-CO_2 requirement as a mechanism for the containment of genetically modified cyanobacteria. *ACS Synth. Biol.* **7**, 384–391 (2018).
38. J. Krissansen-Totton, G. N. Arney, D. C. Catling, Constraining the climate and ocean pH of the early Earth with a geological carbon cycle model. *Proc. Natl. Acad. Sci.* **115**, 4105–4110 (2018).
39. I. Halevy, A. Bachan, The geologic history of seawater pH. *Science* **355**, 1069–1071 (2017).
40. E. A. Laws, B. N. Popp, R. R. Bidigare, M. C. Kennicutt, S. A. Macko, Dependence of phytoplankton carbon isotopic composition on growth rate and $[CO_2]_{aq}$: Theoretical considerations and experimental results. *Geochim. Cosmochim. Acta* **59**, 1131–1138 (1995).
41. B. Kacar, V. Hanson-Smith, Z. R. Adam, N. Boekelheide, Constraining the timing of the Great Oxidation Event within the Rubisco phylogenetic tree. *Geobiology* **15**, 628–640 (2017).
42. P. M. Shih, A. Occhialini, J. C. Cameron, P. J. Andralojc, M. A. J. Parry, C. A. Kerfeld, Biochemical characterization of predicted Precambrian RuBisCO. *Nat. Commun.* **7**, 10382 (2016).
43. M. Lebrato, D. Garbe-Schönberg, M. N. Müller, S. Blanco-Ameijeiras, R. A. Feely, L. Lorenzoni, J.-C. Molinero, K. Bremer, D. O. B. Jones, D. Iglesias-Rodriguez, D. Greeley, M. D. Lamare, A. Paulmier, M. Graco, J. Cartes, J. Barcelos e Ramos, A. de Lara, R. Sanchez-Leal, P. Jimenez, F. E. Paparazzo, S. E. Hartman, U. Westernströer, M. Küter, R. Benavides, A. F. da Silva, S. Bell, C. Payne, S. Olafsdottir, K. Robinson, L. M. Jantunen, A. Korablev, R. J. Webster, E. M. Jones, O. Gilg, P. B. du Bois, J. Beldowski, C. Ashjian, N. D. Yahia, B. Twining, X.-G. Chen, L.-C. Tseng, J.-S. Hwang, H.-U. Dahms, A. Oschlies, Global variability in seawater Mg:Ca and Sr:Ca ratios in the modern ocean. *Proc. Natl. Acad. Sci. U.S.A.* **117**, 22281–22292 (2020).
44. K.-H. Tang, Y. Tang, R. E. Blankenship, Carbon metabolic pathways in phototrophic bacteria and their broader evolutionary implications. *Front. Microbiol.* **2**, 165 (2011).
45. L. C. Kah, R. Riding, Mesoproterozoic carbon dioxide levels inferred from calcified cyanobacteria. *Geology* **35**, 799–802 (2007).
46. G. D. Price, M. R. Badger, F. J. Woodger, B. M. Long, Advances in understanding the cyanobacterial CO_2-concentrating-mechanism (CCM): Functional components, Ci transporters, diversity, genetic regulation and prospects for engineering into plants. *J. Exp. Bot.* **59**, 1441–1461 (2008).
47. H. Bauwe, M. Hagemann, A. R. Fernie, Photorespiration: Players, partners and origin. *Trends Plant Sci.* **15**, 330–336 (2010).
48. A. Bachan, L. R. Kump, The rise of oxygen and siderite oxidation during the Lomagundi Event. *Proc. Natl. Acad. Sci. U.S.A.* **112**, 6562–6567 (2015).
49. S. Kihara, D. A. Hartzler, S. Savikhin, Oxygen concentration inside a functioning photosynthetic cell. *Biophys. J.* **106**, 1882–1889 (2014).
50. G. C. Cannon, C. E. Bradburne, H. C. Aldrich, S. H. Baker, S. Heinhorst, J. M. Shively, Microcompartments in prokaryotes: Carboxysomes and related polyhedra. *Appl. Environ. Microbiol.* **67**, 5351–5361 (2001).
51. A. I. Flamholz, N. Prywes, U. Moran, D. Davidi, Y. M. Bar-On, L. M. Oltrogge, R. Alves, D. Savage, R. Milo, Revisiting trade-offs between Rubisco kinetic parameters. *Biochemistry* **58**, 3365–3376 (2019).
52. J. W. Schopf, Disparate rates, differing fates: Tempo and mode of evolution changed from the Precambrian to the Phanerozoic. *Proc. Natl. Acad. Sci. U.S.A.* **91**, 6735–6742 (1994).
53. E. D. Swanner, A. M. Mloszewska, O. A. Cirpka, R. Schoenberg, K. O. Konhauser, A. Kappler, Modulation of oxygen production in Archaean oceans by episodes of Fe(II) toxicity. *Nat. Geosci.* **8**, 126–130 (2015).
54. A. M. Mloszewska, D. B. Cole, N. J. Planavsky, A. Kappler, D. S. Whitford, G. W. Owttrim, K. O. Konhauser, UV radiation limited the expansion of cyanobacteria in early marine photic environments. *Nat. Commun.* **9**, 3088 (2018).
55. G. J. Dick, S. L. Grim, J. M. Klatt, Controls on O_2 production in cyanobacterial mats and implications for Earth's oxygenation. *Annu. Rev. Earth Planet. Sci.* **46**, 123–147 (2018).
56. A. H. Knoll, R. K. Bambach, Directionality in the history of life: Diffusion from the left wall or repeated scaling of the right? *Paleobiology* **26**, 1–14 (2000).
57. J. Zhang, P. D. Quay, D. O. Wilbur, Carbon isotope fractionation during gas-water exchange and dissolution of CO_2. *Geochim. Cosmochim. Acta* **59**, 107–114 (1995).
58. C. S. Romanek, E. L. Grossman, J. W. Morse, Carbon isotopic fractionation in synthetic aragonite and calcite: Effects of temperature and precipitation rate. *Geochim. Cosmochim. Acta* **56**, 419–430 (1992).
59. T. M. Lenton, S. J. Daines, B. J. W. Mills, COPSE reloaded: An improved model of biogeochemical cycling over Phanerozoic time. *Earth Sci. Rev.* **178**, 1–28 (2018).
60. A. P. Gumsley, K. R. Chamberlain, W. Bleeker, U. Söderlund, M. O. de Kock, E. R. Larsson, A. Bekker, Timing and tempo of the Great Oxidation Event. *Proc. Natl. Acad. Sci.* **114**, 1811–1816 (2017).
61. C. J. Bjerrum, D. E. Canfield, Ocean productivity before about 1.9 Gyr ago limited by phosphorus adsorption onto iron oxides. *Nature* **417**, 159–162 (2002).
62. K. Fennel, M. Follows, P. G. Falkowski, The co-evolution of the nitrogen, carbon and oxygen cycles in the Proterozoic ocean. *Am. J. Sci.* **305**, 526–545 (2005).
63. A. D. Anbar, A. H. Knoll, Proterozoic ocean chemistry and evolution: A Bioinorganic bridge? *Science* **297**, 1137–1142 (2002).
64. D. T. Johnston, F. Wolfe-Simon, A. Pearson, A. H. Knoll, Anoxygenic photosynthesis modulated Proterozoic oxygen and sustained Earth's middle age. *Proc. Natl. Acad. Sci.* **106**, 16925–16929 (2009).
65. N. J. Butterfield, Oxygen, animals and oceanic ventilation: An alternative view. *Geobiology* **7**, 1–7 (2009).
66. P. Sánchez-Baracaldo, A. Ridgwell, J. A. Raven, A Neoproterozoic transition in the marine nitrogen cycle. *Curr. Biol.* **24**, 652–657 (2014).

67. T. L. Hamilton, D. A. Bryant, J. L. Macalady, The role of biology in planetary evolution: Cyanobacterial primary production in low-oxygen Proterozoic oceans. *Environ. Microbiol.* **18**, 325–340 (2016).
68. J. F. Allen, B. Thake, W. F. Martin, Nitrogenase inhibition limited oxygenation of Earth's proterozoic atmosphere. *Trends Plant Sci.* **24**, 1022–1031 (2019).
69. R. E. Summons, J. M. Hayes, Principles of molecular and isotopic biogeochemistry, in *The Proterozoic Biosphere, a Multidisciplinary Study*, J. W. Schopf, C. Klein, Eds. (Cambridge Univ. Press, 1992), pp. 83–94.
70. S. E. Stevens Jr., C. O. P. Patterson, J. Myers, The production of hydrogen peroxide by blue-green algae: A survey[1]. *J. Phycol.* **9**, 427–430 (1973).
71. R. E. Zeebe, D. Wolf-Gladrow, *CO_2 in Seawater: Equilibrium, Kinetics, Isotopes* (Oceanography Series, Elsevier, ed. 1, 2001), vol. 65.
72. C. G. Trick, S. W. Wilhelm, Physiological changes in the coastal marine cyanobacterium *Synechococcus sp.* PCC 7002 exposed to low ferric ion levels. *Mar. Chem.* **50**, 207–217 (1995).
73. R. D. Guy, M. L. Fogel, J. A. Berry, Photosynthetic fractionation of the stable isotopes of oxygen and carbon. *Plant Physiol.* **101**, 37–47 (1993).
74. D. B. McNevin, M. R. Badger, S. M. Whitney, S. von Caemmerer, G. G. B. Tcherkez, G. D. Farquhar, Differences in carbon isotope discrimination of three variants of D-ribulose-1,5-bisphosphate carboxylase/oxygenase reflect differences in their catalytic mechanisms. *J. Biol. Chem.* **282**, 36068–36076 (2007).
75. R. L. Clark, J. C. Cameron, T. W. Root, B. F. Pfleger, Insights into the industrial growth of cyanobacteria from a model of the carbon-concentrating mechanism. *AIChE J.* **60**, 1269–1277 (2014).
76. P. J. Thomas, A. J. Boller, S. Satagopan, F. R. Tabita, C. M. Cavanaugh, K. M. Scott, Isotope discrimination by form IC RubisCO from *Ralstonia eutropha* and *Rhodobacter sphaeroides*, metabolically versatile members of 'Proteobacteria' from aquatic and soil habitats. *Environ. Microbiol.* **21**, 72–80 (2019).
77. E. B. Wilkes, A. Pearson, A general model for carbon isotopes in red-lineage phytoplankton: Interplay between unidirectional processes and fractionation by RubisCO. *Geochim. Cosmochim. Acta* **265**, 163–181 (2019).
78. R. E. Zeebe, On the molecular diffusion coefficients of dissolved CO_2, HCO_3^-, and CO_3^{2-} and their dependence on isotopic mass. *Geochim. Cosmochim. Acta* **75**, 2483–2498 (2011).
79. M. H. O'Leary, Measurement of the isotope fractionation associated with diffusion of carbon dioxide in aqueous solution. *J. Phys. Chem.* **88**, 823–825 (1984).

Acknowledgments: We thank E. Ellison, P. Crockford, and E. Johnson for valuable discussions, J. Jackson and R. Dunbar for editorial handling, and five anonymous reviewers for thoughtful comments. We acknowledge B. Davidheiser-Kroll of the CUBES-SIL for assistance with stable isotope analyses and data reduction. **Funding:** This work was supported by an Agouron Institute postdoctoral fellowship to S.J.H., start-up funding from CU Boulder to B.A.W. and J.C.C., NSF-EF1724393 to B.A.W., NIH T32-GM008759 to N.C.H., and by the U.S. Department of Energy (DOE) DE-SC0019306 to J.C.C. **Author contributions:** S.J.H., B.A.W., and J.C.C. designed the study. S.J.H., C.E.J., and N.C.H. performed the research. S.J.H. and B.A.W. wrote the manuscript with contributions from all authors. **Competing interests:** The authors declare that they have no competing interests. **Data and materials availability:** All data needed to evaluate the conclusions in the paper are present in the paper and/or the Supplementary Materials.

Submitted 20 May 2020
Accepted 11 November 2020
Published 6 January 2021
10.1126/sciadv.abc8998

Citation: S. J. Hurley, B. A. Wing, C. E. Jasper, N. C. Hill, J. C. Cameron, Carbon isotope evidence for the global physiology of Proterozoic cyanobacteria. *Sci. Adv.* **7**, eabc8998 (2021).